Antitumor Agents. 199.† Three-Dimensional Quantitative Structure−Activity Relationship Study of the Colchicine Binding Site Ligands Using Comparative Molecular Field Analysis

Shun-Xiang Zhang,‡ Jun Feng,§ Sheng-Chu Kuo,|| Arnold Brossi,‡ Ernest Hamel,⊥ Alexander Tropsha,*,§ and Kuo-Hsiung Lee*,‡

Natural Products Laboratory and the Laboratory for Molecular Modeling, School of Pharmacy, University of North Carolina at Chapel Hill, Chapel Hill, North Carolina 27599, Graduate Institute of Pharmaceutical Chemistry, China Medical College, Taichung 400, Taiwan, Republic of China, Laboratory of Drug Discovery Research and Development, Developmental Therapeutics Program, Division of Cancer Treatment and Diagnosis, National Cancer Institute, Frederick Cancer Research Center, Frederick, Maryland 21702

Received June 28, 1999

Inhibitors of tubulin polymerization interacting at the colchicine binding site are potential anticancer agents. We have been involved in the synthesis of a number of colchicine site agents, such as thiocolchicinoids and allocolchicinoids, which are colchicine analogues, and 2-phenyl-quinolones and 2-aryl-naphthyridinones, which are the amino analogues of cytotoxic antimitotic flavonoids. The most cytotoxic of the latter compounds strongly inhibit binding of radiolabeled colchicine to tubulin, and these agents therefore probably bind in the colchicine site of tubulin. We have applied conventional CoMFA and q^2-GRS CoMFA to identify the essential structural requirements for increasing the ability of these compounds to form tubulin complexes. The CoMFA model for the training set of 51 compounds yielded cross-validated R^2 (q^2) values of 0.637 for conventional CoMFA and 0.692 for q^2-GRS CoMFA. The predictive power of this model was confirmed by successful activity prediction for a test set of 53 compounds with known potencies as inhibitors of tubulin polymerization. The activities of 88% of the compounds were predicted with absolute value of residuals of less than 0.5. The predictive q^2 values were 0.546 for conventional CoMFA and 0.426 for q^2-GRS CoMFA. The conventional CoMFA model with the highest predictive q^2 (0.546) was analyzed in detail in terms of underlying structure−activity relationships.

Introduction

The microtubule system of eukaryotic cells is an attractive target for the development of anticancer chemotherapeutic agents. Microtubules are highly dynamic organelles that are essential in mitosis.[2] Chemicals that attack microtubules through tubulin, their major structural component, disrupt or suppress both microtubule structure and normal functions by inhibition or promotion of microtubule assembly. This action results in cell arrest in mitosis.[3] Examples of clinically used antimitotic agents are the vinca alkaloids,[4] which inhibit microtubule polymerization, and taxoids,[5] which promote microtubule assembly. Colchicine is another important antimitotic agent. Although it has limited medicinal application due to its high toxicity, colchicine has played a fundamental role in elucidation of the properties and functions of tubulin and microtubules.[6] Many natural products, such as cornigerine,[7] podophyllotoxin,[8] steganacin,[9] combretastatin,[10,11] and flavonols,[12] bind to the colchicine site. Structurally, the compounds binding to this site are much simpler than those binding to vinca alkaloid or taxol domains. These compounds generally share "homology" with the A- and C-rings of colchicine. This common feature has been described as a "biaryl" system connected by a hydrocarbon bridge of variable length.[13,14] Over the years, we have been involved in the synthesis of a number of colchicine binding site agents, such as thiocolchicinoids and allocolchicinoids, which are colchicine analogues,[15−20] and 2-phenyl-quinolones and 2-aryl-naphthyridinones, which are the amino analogues of cytotoxic antimitotic flavonoids.[21−28] The most cytotoxic compounds in these groups showed potent inhibitory effects in vitro on tubulin polymerization and appear to interact at the colchicine binding site of tubulin. The efforts toward the development of tubulin inhibitors were recently reviewed by Shi and Lee.[29]

As the numbers of active derivatives increase, the formulation of a useful SAR becomes increasingly difficult. Thus, molecular models should be developed that can better interpret pharmacological data and predict novel biologically active compounds. Ligand-based methods of analysis, such as pharmacophore mapping and quantitative structure activity relationships (QSAR), remain the major approach for developing predictive correlations between ligand structure and activity. Previously, ter Haar et al. performed a QSAR study on colchicine site agents by multiCASE/CASE analyses, but the results were poorly interpretable and did not give structural information about the binding site.[30] In this

† For Part 198, see ref 1.
* To whom correspondence should be addressed.
‡ Natural Products Laboratory, University of North Carolina at Chapel Hill.
§ Laboratory for Molecular Modeling, University of North Carolina at Chapel Hill.
|| China Medical College.
⊥ Laboratory of Drug Discovery Research and Development, NCI.

10.1021/jm990333a CCC: $19.00
Published on Web 01/06/2000

Chart 1. Structures of 2-Aryl-1,8-naphthyridin-4-ones (**1**−**50**)[a]

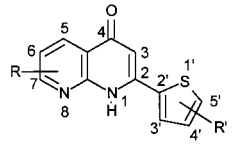

1 $R_6 = CH_3$, $R_3' = CH_3$
2* $R_6 = CH_3$, $R_5' = CH_3$
3* $R_7 = CH_3$, $R_3' = CH_3$
4 $R_7 = CH_3$, $R_5' = Cl$
5 $R_7 = CH_3$, $R_5' = Br$
6 $R_7 = CH_3$, $R_5' = CH_3$
7 $R_7 = CH_3$, $R_5' = H$

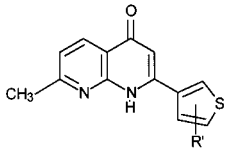

8 $R'_2 = R'_5 = H$
9* $R'_2 = R'_5 = CH_3$

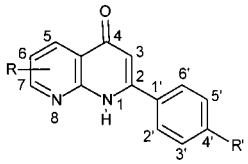

10 $R_5 = CH_3$, $R' = F$
11 $R_5 = CH_3$, $R' = OCH_3$
12 $R_5 = CH_3$, $R' = Cl$
13* $R_5 = CH_3$, $R' = CH_3$
14* $R_5 = R_7 = CH_3$, $R' = CH_3$
15 $R_6 = CH_3$, $R' = CH_3$
16* $R_6 = CH_3$, $R' = OCH_3$
17* $R_6 = CH_3$, $R' = Cl$
18 $R_6 = Cl$, $R' = F$
19 $R_7 = CH_3$, $R' = Cl$
20* $R_7 = CH_3$, $R' = CH_3$

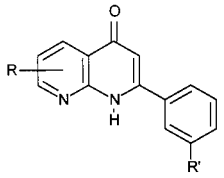

22 $R_4 = CH_3$, $R' = CH_3$
23 $R_4 = CH_3$, $R' = OCH_3$
24* $R_4 = CH_3$, $R' = Cl$
25 $R_5 = R_7 = CH_3$, $R' = Cl$
26 $R_5 = R_7 = CH_3$, $R' = OCH_3$
27* $R_5 = R_7 = CH_3$, $R' = F$
28 $R_6 = CH_3$, $R' = F$
29 $R_6 = CH_3$, $R' = Cl$
30 $R_6 = CH_3$, $R' = OCH_3$
31* $R_6 = CH_3$, $R' = CH_3$
32 $R_7 = CH_3$, $R' = F$
33 $R_7 = CH_3$, $R' = CH_3$
34* $R_7 = CH_3$, $R' = Cl$
35* $R_7 = CH_3$, $R' = OCH_3$
36 R = H, R' = Cl
37 R = H, R' = OCH_3
38* R = H, R' = CH_3
39 R = Br, R' = OCH_3
40* R = Cl, R' = OCH_3

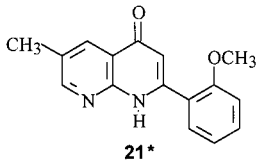

21*

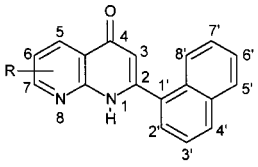

41 $R_5 = CH_3$
42* $R_6 = CH_3$
43 $R_7 = CH_3$
44* $R_5 = R_7 = CH_3$
45* R = H

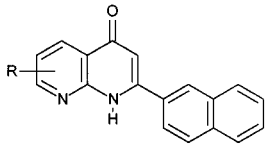

46* $R_5 = CH_3$
47 $R_6 = CH_3$
48* $R_6 = Cl$
49 $R_7 = CH_3$
50* R = H

[a] Asterisk (*) indicates compounds in test set.

paper, we report the development of a three-dimensional quantitative structure−activity relationship (3D QSAR) of 104 colchicine binding site agents including thiocolchicinoids, quinolones, and naphthyridinones, using comparative molecular field analysis (CoMFA)[33] and a CoMFA/q^2-GRS technique developed by Cho and Tropsha.[31] Our goals were to enhance our knowledge regarding the molecular recognition of tubulin polymerization inhibitors and to help design more effective inhibitors against this crucial anticancer target. We have obtained highly predictive QSAR models with a training set of 51 compounds using conventional CoMFA and q^2-GRS/CoMFA methods as indicated by the q^2 values. The cross-validation R^2 (q^2) values are 0.637 and 0.693 for conventional CoMFA and q^2-GRS/CoMFA, respectively.

Data Set and Biological Activity

Data obtained with 104 colchicine site compounds were included in this study. The molecules were classified into four families, based on their chemical structure: colchicinoids and thiocolchicinoids, allocolchinoids, 2-phenyl-4-quinolones, and 2-aryl-1,8-naphthyridinones (Charts 1−4). Inhibition of tubulin polymerization was expressed as IC_{50} (μM) values, which represents the drug concentration that caused 50% inhibition of the extent of tubulin polymerization. The $\log(1/IC_{50})$ (pIC_{50}) values were used to derive 3D QSAR models and are listed in Tables 1 and 2.[15−19,21−28,32]

One goal of this study was to test the predictability of CoMFA analysis. Great structural diversity is necessary to obtain meaningful results from 3D QSAR study using the CoMFA method.[33] To carry out this study, we divided the compounds into a training set containing 51 compounds (Table 1) and a test set of 53 compounds (Table 2) in order to assess the predictive power of the model. These sets contained compounds from all families and represented a balanced number of both the more active and the less active compounds. We divided all compounds into several groups according to their activities. In each group, the compounds of every family were split between training and test sets randomly.

Conventional CoMFA

Structures were generated and CoMFA was performed within the QSAR option of SYBYL molecular modeling software.[34] Default settings were used except as otherwise noted. Molecular mechanics calculations were performed with the standard Tripos force field, with a convergence criterion requiring a minimum energy change of 0.05 kcal/mol. Charge calculations were done using the Gasteiger−Huckel method as implemented in Sybyl. The steric and electrostatic field energies were calculated using sp^3 carbon probe atoms with +1 charge. Low-energy conformers were obtained via the SYBYL random search method. The CoMFA QSAR equations were calculated using the partial least-

Chart 2. Structures of 2-Phenyl-quinolones and 2,3-Dihydro-2-phenyl-4-quinolinones (**51**−**66**)[a]

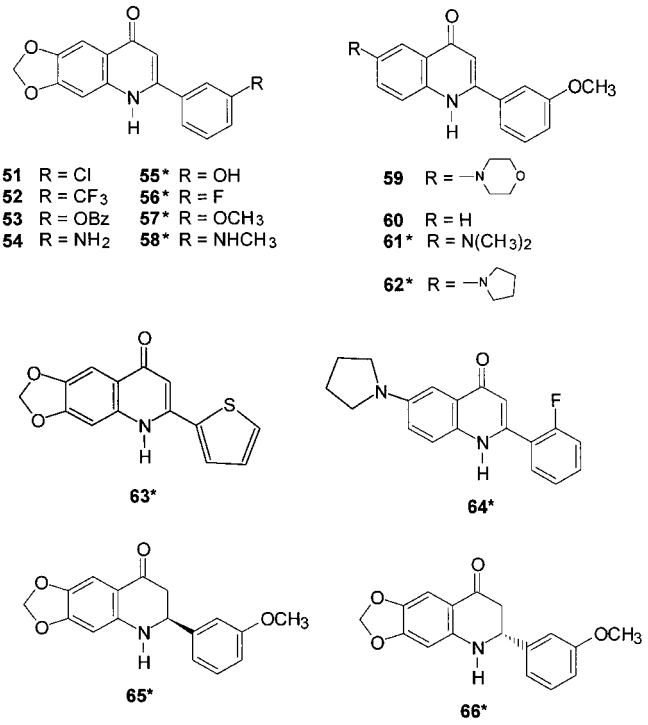

[a] Asterisk (*) indicates compounds in test set.

squares (PLS) algorithm. The optional number of components (ONC) in the final PLS model was determined by the cross-validated R^2 (q^2) and standard error of prediction (SDEP) values, as obtained from the leave-one-out cross-validation technique. The q^2 value was calculated from the following standard equation

$$q^2 = (\mathrm{SD} - \mathrm{PRESS})/\mathrm{SD}$$

in which "SD" is the variance of the biological activities of the molecules around the mean value. "PRESS" represents the sum of the squared differences between the predicted and actual target property values for every compound. The number of components with the lowest SDEP value was selected as the ONC. All calculations were performed on a Silicon Graphics Octane workstation.

Structure Alignment

The geometry of each compound was optimized individually with the Tripos force field, with no constraints on the internal geometry of the molecules. *aR*,7*S*-Colchicine (**67**),[39−40] a ring-constrained natural product, was chosen as the template molecule due to its rigidity and relatively high affinity for tubulin. Each compound was aligned to the template molecule by performing a random conformational search and rms-fitting the pharmacophoric atoms of each conformer to those of the template. The conformer with the lowest rms value (as fitted to the template) was retained in its superimposed position. In the 2-phenyl-4-quinolone and 2-aryl-1,8-naphthyridinone groups, the compounds possessed a freely rotatable aryl ring (C-ring), and the Modify Torsion command within Sybyl was used to generate a conformation that mimicked the orientation of the A- and C-rings of the template molecule.

Structural alignment for CoMFA and q^2-GRS is dependent upon a rational identification of the pharmacophore of each compound in the data set. Because all colchicine binding site agents share a "biaryl" system,[13,14] the two aryl rings should be fitted for all compounds, assuming that all compounds interact at the same binding site at the receptor level. We have attempted two alignment rules. In alignment 1, the "biaryl" feature was selected for alignment of all compounds. Three atoms of the aromatic ring including the carbons constituting the "biaryl" A/C-ring linkage (C-1a, -1, -2, and -12a in colchicinoids and thiocolchicinoids;

Chart 3. Structures of Colchicine and Thiocolchicine Derivatives (**67**−**84**)[a]

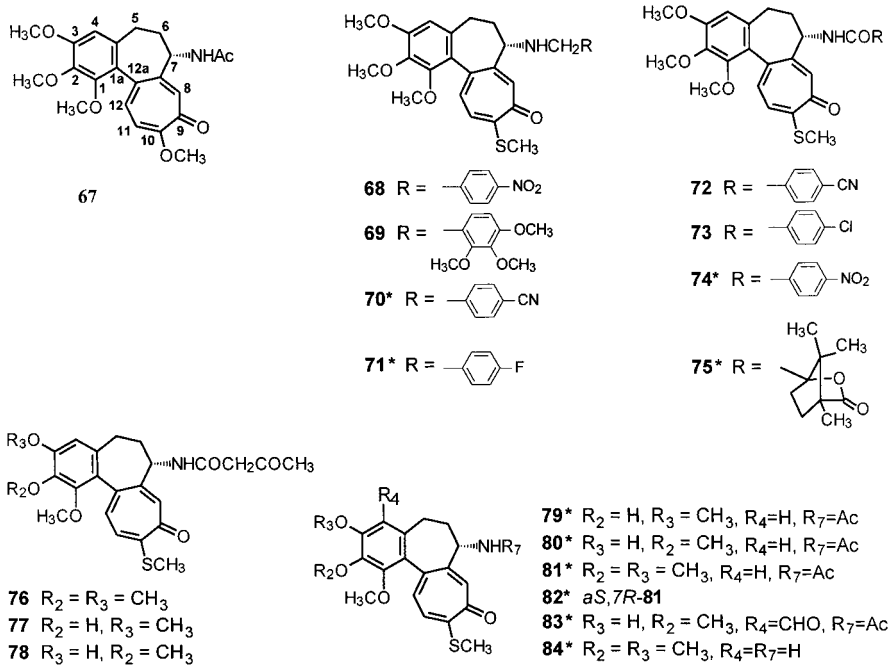

[a] Asterisk (*) indicates compounds in test set.

Chart 4. Structures Deacetamidothiocolchicin-7-ol and Its Esters, Six-Membered B-Ring Thiocolchicinoids, and Allocolcinoids (**85**−**104**)[a]

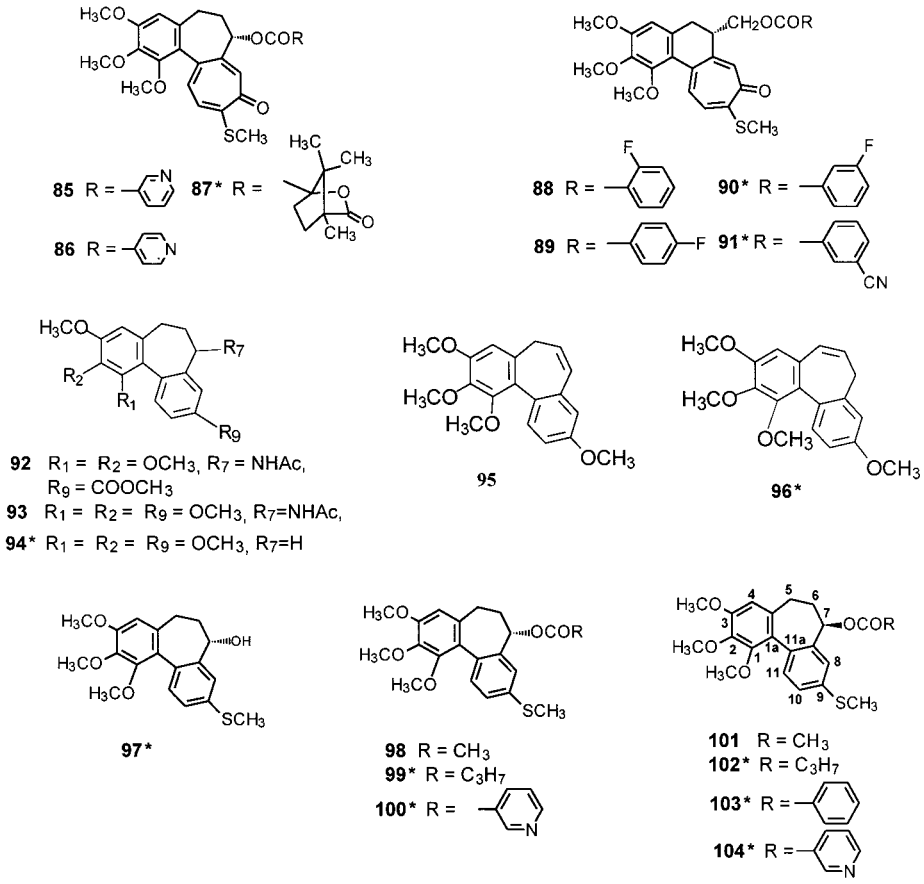

[a] Asterisk (*) indicates compounds in test set.

C-1a, -1, -2, and -11a in allocolchicinoids; C-1′, -2′, -3′, and -2 in quinolones and naphthyridinones) were fitted to C-1a, -1, -2, and -12a of *aR*,7*S*-colchicine (**67**), respectively. In alignment 2, the same carbons were selected as in alignment 1, except for the *aS*,7*R*-thiocolchicinoids and allocolchicinoids (**82**, **101**, **102**, **103**, **104**). For these five compounds, C-11a, -11, -10, and -1a in compounds **101**−**104**, and C-12a, -12, -11, and -1a in compound **82** were fitted to C-1a, -1, -2, and -12a of *aR*,7*S*-colchicine (**67**), respectively. The rationale of this alignment will be discussed below.

q²-GRS Routine. The q²-GRS process has been described in detail elsewhere.[31,35] The application of this method leads to reproducible q^2 values that do not depend on the global orientation of the aligned molecules on the user terminal. The q²-GRS procedure is performed as follows. Step 1: Conventional CoMFA is performed, initially using an automatically generated region file (a rectangular grid). Step 2: The rectangular grid, encompassing aligned molecules, is then divided into 125 small boxes of equal size, and the Cartesian coordinates of the upper right and lower left corners of each box are calculated. Step 3: For each of these newly generated region files, a separate CoMFA is performed with a step size of 1.0 Å. Step 4: The regions with the q^2 value greater than the specified cutoff are selected for further analysis. Step 5: The selected regions are combined to generate a master region file. Step 6: The final CoMFA is performed using the master region file.

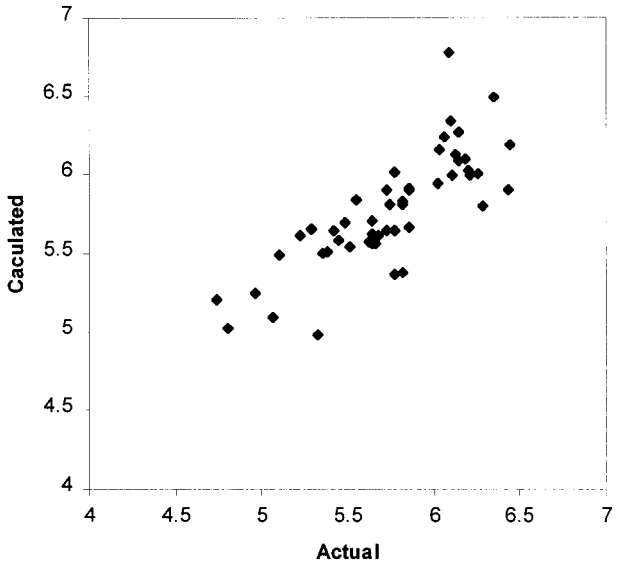

Figure 1. Actual vs calculated values in training set using alignment 2 by conventional CoMFA.

Results and Discussion

Tables 1 and 2 list predicted vs actual biological values[15−19,21−28,32] for each compound, as determined by each type of QSAR analysis. Figures 1 and 2 show plots of predicted vs actual activity for both training and test sets. We have aligned the compounds using our current knowledge of the binding complexes of tubulin and

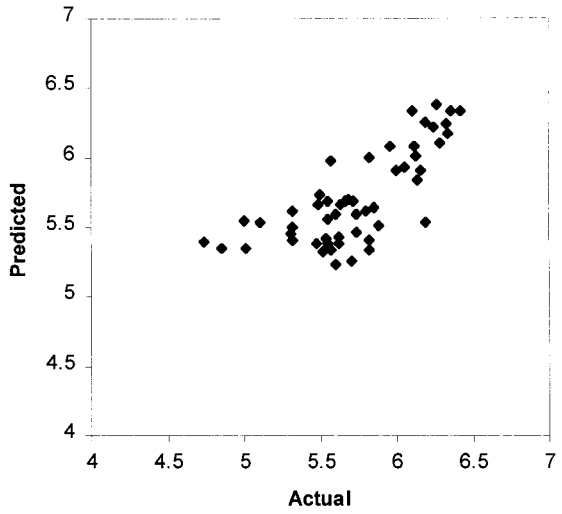

Figure 2. Actual vs calculated values in test set using alignment 2 by conventional CoMFA.

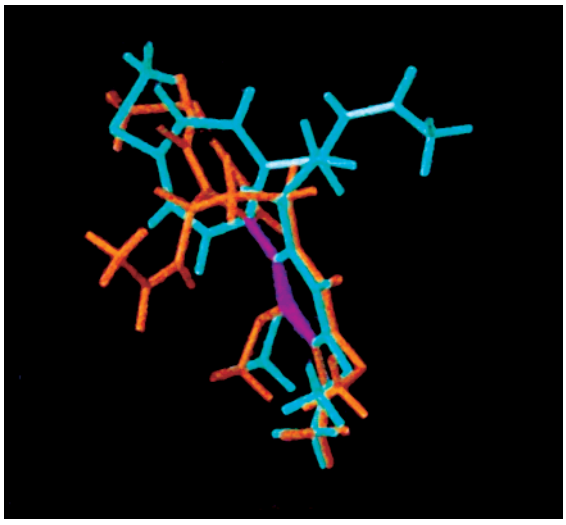

Figure 3. Alignment 1 of compounds **67** (cyan) and **82** (orange). Alignment bonds shown in violet. The side chains of the compounds are located on different sides.

colchicine (**67**). Colchicine can exist in two configurations: (−) *aR*,7*S*-colchicine (**67**)[39,40] and (+) *aS*,7*R*-colchicine. The lowest energy conformations of these isomers differ from one another in the dihedral angle of the A- and C-rings.[36−38] The conformational analysis of the (*aR*,7*S*) and (*aS*,7*R*) forms of the colchicine ring system demonstrated that only those colchicinoids with the proper stereochemical arrangement of the A- and C-rings bind with high affinity in the colchicine site on tubulin. To model the colchicine site, we have developed two alignment models. Alignment 1 did not consider the different dihedral angles of the A- and C-rings between the (*aR*,7*S*) and (*aS*,7*R*) forms and direction of the side chain. Alignment 2 altered the alignment for the *aS*,7*R* form, which closely meets the structural and spatial requirements of the colchicine binding site on tubulin, causing the side chain to be located on the same side as the *aR*,7*S* form compounds (Figures 3 and 4). In the training set, only compound **101** has the *aS*,7*R* form; however, the absolute residual value reduced significantly from 0.11 for alignment 1 to 0.03 for alignment 2, for the conventional CoMFA, and from 0.70 to 0.32 for the q^2-GRS CoMFA. Alignment 2 also improved the

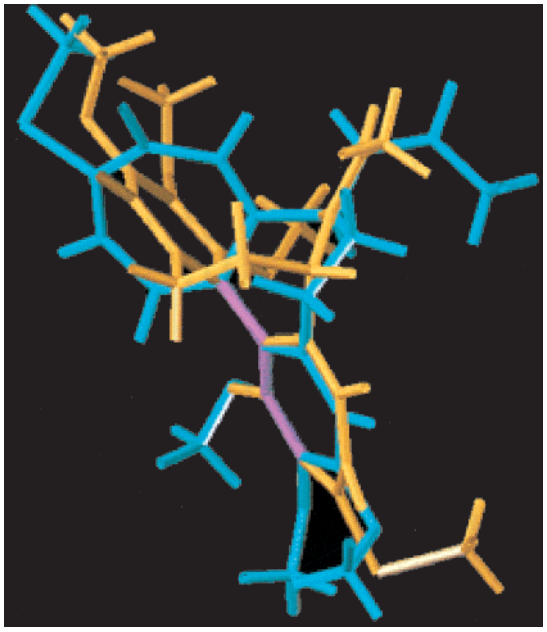

Figure 4. Alignment 2 of compounds **67** (cyan) and **82** (orange). Alignment bonds shown in violet. The side chains of the compounds are located on the same side.

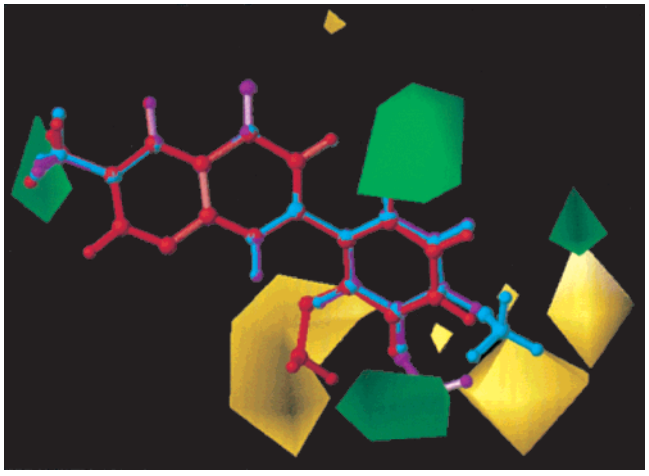

Figure 5. Steric fields generated with conventional CoMFA, with compounds **16** (cyan), **21** (red), and **30** (purple) as representative inhibitors: yellow indicates regions predicted to cause unfavorable steric interactions of bulky substituents with the receptor; green indicates regions where bulky substituents are predicted to improve affinity for the receptor.

cross-validated R^2 (q^2) from 0.626 to 0.637 in the conventional CoMFA and from 0.674 to 0.692 in the q^2-GRS CoMFA. The key statistical parameters associated with these CoMFA models are shown in Table 3. Alignment 2 showed better correlation than alignment 1 for both CoMFA methods. For alignment 2, the cross-validated R^2 (q^2) was 0.637 with an optimal number of components (ONC) of 6. With a cutoff value of 0.1, the q^2-GRS CoMFA improved the final q^2 significantly with all different numbers of components. The best q^2 was 0.692 with an ONC of 8. The non-cross-validated R^2 resulting from q^2-GRS CoMFA fields was 0.958 with an ONC of 8. This alignment was selected to construct the steric and electrostatic contours (Figures 5−7). A model with $q^2 \geq 0.5$ is generally regarded as internally predictive, thus the q^2 values obtained in the present case impart credibility to our CoMFA models.

Table 1. CoMFA Actual and Calculated Activities for Training Set Molecules

		alignment 1				alignment 2			
		conventional		q^2-GRS		conventional		q^2-GRS	
compd	actual	calcd	residual	calcd	residual	calcd	residual	calcd	residual
1	5.42	5.63	−0.21	5.29	0.13	5.64	−0.22	5.29	0.13
4	5.77	5.38	0.39	5.63	0.14	5.37	0.4	5.61	0.16
5	5.82	5.39	0.43	5.77	0.05	5.38	0.44	5.73	0.09
6	5.77	6.00	−0.23	6.18	−0.41	6.01	−0.24	6.16	−0.39
7	5.22	5.62	−0.4	5.54	−0.32	5.61	−0.39	5.53	−0.31
8	5.10	5.51	−0.41	5.22	−0.12	5.49	−0.39	5.21	−0.11
10	4.74	5.22	−0.48	4.96	−0.22	5.20	−0.46	4.91	−0.17
11	5.06	5.06	0	5.01	0.05	5.09	−0.03	4.97	0.09
12	5.32	4.99	0.33	4.95	0.37	4.98	0.34	4.95	0.37
15	5.62	5.56	0.06	5.48	0.14	5.57	0.05	5.40	0.22
18	4.80	5.03	−0.23	4.68	0.12	5.02	−0.22	4.76	0.04
19	4.96	5.26	−0.3	5.4	−0.44	5.25	−0.29	5.34	−0.38
22	5.74	5.80	−0.06	5.68	0.06	5.81	−0.07	5.66	0.08
23	6.21	5.98	0.23	5.9	0.31	5.99	0.22	5.93	0.28
25	6.11	5.98	0.13	6	0.11	5.99	0.12	5.99	0.12
26	6.06	6.23	−0.17	5.99	0.07	6.23	−0.17	6.02	0.04
28	6.20	5.98	0.22	6.38	−0.18	6.02	0.18	6.36	−0.16
29	6.14	6.04	0.1	6.17	−0.03	6.08	0.06	6.12	0.02
30	6.10	6.30	−0.2	6.29	−0.19	6.34	−0.24	6.20	−0.1
32	6.28	5.80	0.48	5.95	0.33	5.8	0.48	6.09	0.19
33	5.72	5.90	−0.18	5.72	0	5.9	−0.18	5.78	−0.06
36	5.82	5.80	0.02	6.13	−0.31	5.81	0.01	6.1	−0.28
37	6.02	5.93	0.09	5.97	0.05	5.94	0.08	5.96	0.06
39	5.82	5.81	0.01	6.09	−0.27	5.81	0.01	5.99	−0.17
41	6.03	6.14	−0.11	6.27	−0.24	6.15	−0.12	6.16	−0.13
43	6.18	6.08	0.1	6.01	0.17	6.09	0.09	6.03	0.15
47	5.68	5.60	0.08	5.36	0.32	5.61	0.07	5.38	0.3
49	5.29	5.66	−0.37	5.57	−0.28	5.65	−0.36	5.60	−0.31
51	6.43	5.92	0.51	6.07	0.36	5.9	0.53	6.10	0.33
52	6.09	6.75	−0.66	6.73	−0.64	6.78	−0.69	6.65	−0.56
53	6.35	6.50	−0.15	6.38	−0.03	6.49	−0.14	6.27	0.08
54	6.14	6.23	−0.09	6.28	−0.14	6.27	−0.13	6.19	−0.05
59	6.44	6.16	0.28	6.18	0.26	6.18	0.26	6.23	0.21
60	5.85	5.89	−0.04	6.12	−0.27	5.9	−0.05	6.06	−0.21
67	5.38	5.71	−0.33	5.54	−0.16	5.51	−0.13	5.74	−0.36
68	5.64	5.57	0.07	5.66	−0.02	5.56	0.08	5.65	−0.01
69	5.64	5.67	−0.03	5.55	0.09	5.7	−0.06	5.61	0.03
72	5.72	5.63	0.09	5.61	0.11	5.64	0.08	5.66	0.06
73	5.64	5.60	0.04	5.65	−0.01	5.62	0.02	5.67	−0.03
76	5.85	5.62	0.23	5.61	0.24	5.66	0.19	5.62	0.23
77	5.48	5.70	−0.22	5.75	−0.27	5.69	−0.21	5.74	−0.26
78	5.77	5.60	0.17	5.74	0.03	5.64	0.13	5.77	0
85	6.12	6.17	−0.05	6.00	0.12	6.12	0	6.00	0.12
86	6.25	6.07	0.18	6.12	0.13	6	0.25	6.06	0.19
88	5.44	5.56	−0.12	5.57	−0.13	5.58	−0.14	5.55	−0.11
89	5.35	5.53	−0.18	5.37	−0.02	5.50	−0.15	5.30	0.05
92	5.85	5.91	−0.06	5.81	0.04	5.91	−0.06	5.65	0.2
93	5.82	5.86	−0.04	5.70	0.12	5.83	−0.01	5.90	−0.08
95	5.66	5.57	0.09	5.33	0.33	5.56	0.1	5.40	0.26
98	5.55	5.84	−0.29	6.00	−0.45	5.84	−0.29	6.26	−0.71
101	5.51	5.62	−0.11	6.21	−0.7	5.54	−0.03	5.83	−0.32

To validate our model, we attempted to predict the inhibitory activity against tubulin polymerization for the 53 ligands of the test set. The predicted pIC_{50} values for these 53 compounds as well as residual values are given in Table 2. The pIC_{50} values of 62% of the compounds were predicted with an absolute value of residuals less than 0.2, while for 88% of the compounds the pIC_{50} values were predicted with this value less than 0.5. The predicted q^2 values were obtained and are shown in Table 3. As with the training set, alignment 2 improved the predictive q^2 relative to alignment 1 for conventional CoMFA, but not for q^2-GRS CoMFA. Possibly, the molecules in the data set possess structural features that translate into 3D molecular field descriptors insensitive to the region-selection procedure of the q^2-GRS analysis, especially for the *aS*,7*R*-thiocolchicinoids and allocolchicinoids (**82**, **102**−**104**) and for the new chemical class in the test set, compounds **65** and **66**. Because conventional CoMFA with alignment 2 gave the highest predictive q^2 (0.546), we decided to use this model for further evaluation.

The CoMFA steric and electrostatic fields were obtained using an sp^3 carbon with +1 charge. Figures 5−7 illustrate steric and electrostatic fields generated by CoMFA. The steric and electrostatic fields were analyzed for areas that might improve binding affinity with changes in substituent charges or sizes. The green (sterically favorable) and yellow (sterically unfavorable) contours shown in Figures 5 and 6 represent 80% and 20% level contributions, respectively. These contours adequately represent trends in structure−activity relationship for both training and test set compounds. In the 2-thienyl-1,8-naphthyridin-4-one series (**1**, **4**−**8** in training set, and **2**, **3**, and **9** in test set), the yellow

Table 2. CoMFA Actual and Predicted Activities for Test Set Molecules

		alignment 1				alignment 2			
		conventional		q^2-GRS		conventional		q^2-GRS	
compd	actual	predicted	residual	predicted	residual	predicted	residual	predicted	residual
2	5.57	6.04	−0.47	5.84	−0.27	5.97	−0.4	5.88	−0.31
3	5.55	5.33	0.22	5.30	0.25	5.38	0.17	5.37	0.18
9	5.32	5.45	−0.13	5.49	−0.17	5.50	−0.18	5.60	−0.28
13	5.54	5.40	0.14	5.47	0.07	5.42	0.12	5.48	0.06
14	5.00	5.55	−0.55	5.51	−0.51	5.55	−0.55	5.53	−0.53
16	5.11	5.53	−0.42	5.23	−0.12	5.53	−0.42	5.13	−0.02
17	5.70	5.24	0.46	5.29	0.41	5.26	0.44	5.26	0.44
20	5.31	5.45	−0.14	5.44	−0.13	5.45	−0.14	5.49	−0.18
21	4.74	5.33	−0.59	5.50	−0.76	5.40	−0.66	5.44	−0.7
24	6.00	5.91	0.09	6.02	−0.02	5.90	0.1	5.99	0.01
27	6.13	6.07	0.06	6.17	−0.04	6.01	0.12	6.19	−0.06
31	5.82	5.97	−0.15	5.90	−0.08	6.00	−0.18	5.91	−0.09
34	6.05	5.96	0.09	6.03	0.02	5.93	0.12	6.04	0.01
35	6.12	6.10	0.02	5.98	0.14	6.08	0.04	6.02	0.1
38	5.48	5.63	−0.15	5.67	−0.19	5.66	−0.18	5.70	−0.22
40	6.14	5.84	0.3	5.94	0.2	5.84	0.3	5.95	0.19
42	6.26	6.40	−0.14	6.24	0.02	6.38	−0.12	6.21	0.05
44	6.11	6.33	−0.22	6.14	−0.03	6.33	−0.22	6.13	−0.02
45	5.96	6.08	−0.12	6.06	−0.1	6.08	−0.12	6.07	−0.11
46	5.74	5.41	0.33	5.41	0.33	5.47	0.27	5.39	0.35
48	5.60	5.18	0.42	5.31	0.29	5.24	0.36	5.33	0.27
50	4.85	5.30	−0.45	5.37	−0.52	5.35	−0.5	5.36	−0.51
55	6.33	6.21	0.12	6.31	0.02	6.24	0.09	6.25	0.08
56	6.28	6.11	0.17	6.38	−0.1	6.10	0.18	6.40	−0.12
57	6.24	6.18	0.06	6.33	−0.09	6.22	0.02	6.21	0.03
58	6.19	6.21	−0.02	6.19	0	6.25	−0.06	6.10	0.09
61	6.42	6.31	0.11	6.28	0.14	6.33	0.09	6.37	0.05
62	6.36	6.32	0.04	6.32	0.04	6.33	0.03	6.41	−0.05
63	5.66	5.66	0	5.61	0.05	5.69	−0.03	5.55	0.11
64	6.34	6.18	0.16	6.03	0.31	6.17	0.17	6.11	0.23
65	6.16	5.84	0.32	6.09	0.07	5.90	0.26	5.96	0.2
66	5.63	5.72	−0.09	6.04	−0.41	5.66	−0.03	5.93	−0.3
70	5.60	5.55	0.05	5.58	0.02	5.59	0.01	5.65	−0.05
71	5.49	5.71	−0.22	5.64	−0.15	5.73	−0.24	5.69	−0.2
74	5.68	5.60	0.08	5.65	0.03	5.70	−0.02	5.65	0.03
75	5.62	5.49	0.13	5.33	0.29	5.43	0.19	5.44	0.18
79	5.82	5.44	0.38	5.37	0.45	5.41	0.41	5.29	0.53
80	5.80	5.64	0.16	5.59	0.21	5.62	0.18	5.62	0.18
81	6.19	5.55	0.64	5.55	0.64	5.53	0.66	5.52	0.67
82	5.01	5.91	−0.9	5.88	−0.87	5.35	−0.34	6.19	−1.18
83	5.55	5.73	−0.18	5.92	−0.37	5.68	−0.13	5.73	−0.18
84	5.88	5.49	0.39	5.59	0.29	5.51	0.37	5.55	0.33
87	5.85	5.54	0.31	5.82	0.03	5.64	0.21	5.70	0.15
90	5.47	5.33	0.14	5.31	0.16	5.38	0.09	5.37	0.1
91	5.52	5.29	0.23	5.32	0.2	5.33	0.19	5.37	0.15
94	5.72	5.73	−0.01	5.51	0.21	5.68	0.04	5.62	0.1
96	5.82	5.39	0.43	5.31	0.51	5.34	0.48	5.40	0.42
97	5.74	5.62	0.12	5.58	0.16	5.59	0.15	5.63	0.11
99	5.55	5.60	−0.05	5.57	−0.02	5.56	−0.01	5.52	0.03
101	5.32	5.64	−0.32	5.57	−0.25	5.61	−0.29	5.55	−0.23
102	5.32	5.35	−0.03	5.75	−0.43	5.41	−0.09	5.43	−0.11
103	5.57	5.38	0.19	5.74	−0.17	5.34	0.23	5.41	0.16
104	5.62	5.40	0.22	5.74	−0.12	5.38	0.24	5.38	0.24

Table 3. Statistical Data for QSAR Method Results

	alignment 1		alignment 2	
	conventional	q^2-GRS	conventional	q^2-GRS
CV−R^2 (q^2)	0.626	0.674	0.637	0.692
optimal number of components	6	6	6	8
standard error	0.267	0.249	0.263	0.248
non-CV−R^2	0.884	0.941	0.888	0.958
F value	12.29	53.8	12.89	121.2
steric contribution	0.466	0.409	0.461	0.408
electrostatic contribution	0.534	0.591	0.539	0.592
predictive q^2	0.461	0.4572	0.546	0.426

region at the bottom left corresponds to steric factors exhibited by the 3′-methyl group of 2-α-thienyl compounds and the 2′-methyl group of 2-β-thienyl compounds. The green region at the upper right corresponds to the steric factor exhibited by the 5′-methyl group of 2-α-thienyl compounds. In the 2-α-thienyl series, compounds with a 5′-methyl group had higher inhibitory activity than those with a 3′-methyl. In the 2-phenyl-1,8-naphthyridin-4-one series, the green region at the bottom corresponds to the steric factor exhibited by the 3′-methyl/methoxy group in the more active compounds **23**, **26**, **30**, **33**, and **37** (in the training set) and **31**, **35**, and **38** (in the test set). The 2′-methyl/methoxy groups in compounds **11** and **15** (in the training set) and **13**, **14**, **16**, **20**, and **21** (in the test set) were located in two yellow regions, representing reduced or disrupted affinity (shown in Figure 5). The 2-α-naphthyl group in

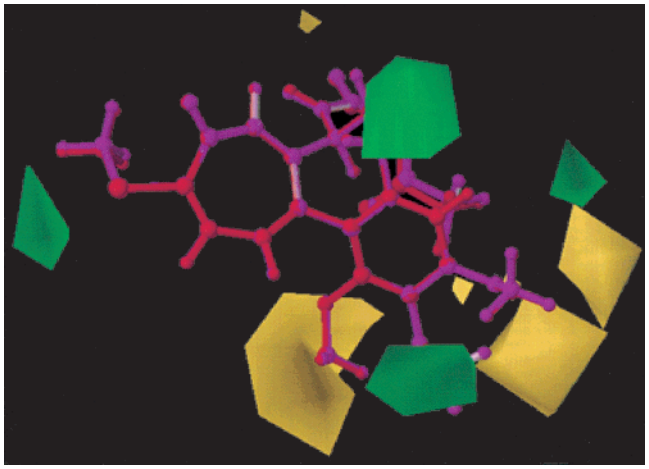

Figure 6. Steric fields generated with conventional CoMFA, with compounds **76** (purple) and **77** (red) as representative inhibitors: yellow indicates regions predicted to cause unfavorable steric interactions of bulky substituents with the receptor; green indicates regions where bulky substituents are predicted to improve affinity for the receptor.

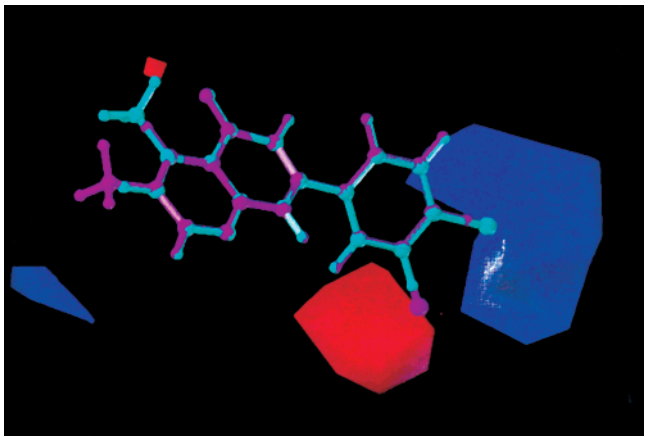

Figure 7. Electrostatic fields generated with conventional CoMFA, with compounds **12** (cyan) and **29** (purple) as a representative inhibitors: blue indicates regions where more positively charged substituents are predicted to improve affinity; red indicates regions where more negatively charged substituents are predicted to improve affinity.

compounds **41** and **43** (in the training set) and **42**, **44**–**46**, **48**, and **50** (in the test set) was located in the upper green region, associated with higher affinity. The 2-*β*-naphthyl group in compounds **47** and **49** (in the training set) and **46**, **48**, and **50** (in the test set) filled the right yellow region, associated with lower affinity. In the thiocolchicinoids and allocolchicinoids, most of the steric fields surrounded the A-ring and indicated that this ring should play a critical role in the active compounds. The 2-methoxy group was located in the green region at the bottom, indicative of the increasing affinity among compounds **76** and **77** (shown in Figure 6). The B-ring and the side chain in those series play an important role in keeping the A- and C-ring biaryl conformation suitable for tubulin binding and preventing isomerization to inactive isomers. However, size is not critical for tubulin binding. Our CoMFA model confirms these observations because few fields surround the B-ring and the side chain. Similar results were observed with 2-phenyl 4-quinolones.

Chart 5. Proposed Compound Model and a Newly Designed Compound

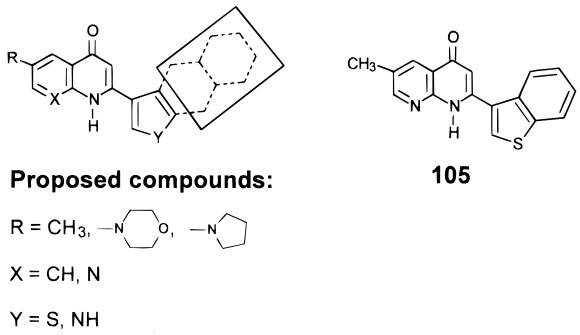

Figure 7 shows CoMFA electrostatic fields, with blue regions indicative of areas where affinity could be improved by more positively charged substituents. Red regions are indicative of areas where affinity could be improved by more negatively charged substituents. The blue and red contours shown in Figure 7 represent 80% and 20% level contributions, respectively. The red regions surrounding the 3′-substituent are consistent with the observation that the binding affinities improve in the following order with 3′-halogen substituents: F > Cl > Br, as observed in compounds **25**, **29**, **32**, **36**, and **39** in the training set, and **24**, **27**, **34**, and **40** in the test set. The blue regions surrounding the 4′-substituent agree with the observation that the binding affinity with a 4′-F was less than with a 4′-Cl, as observed in compounds **10**, **12**, **18**, and **19** in the training set and **17** in the test set (shown in Figure 7).

Summary and Prospectus

We have investigated the colchicine binding site of the proposed composite pharmacophore of 104 colchicine binding site agents using the CoMFA/q^2-GRS approach. We found that the CoMFA model explains experimental SAR trends for these compounds obtained previously. Generally, the active compounds fit into the favorable steric field better than the inactive ones. The less active compounds either did not fill the favorable regions well or they extended into the unfavorable regions. Most of the steric and electrostatic fields surrounded the A-ring of colchicinoids/thicolchicinoids and the C-ring of quinolones/naphthyridinones, indicating that these groups play critical roles in the active affinities. This observation agreed with the previous results that the colchicine binding site on tubulin has very stringent structural and spatial requirements[29] and, in the naphthyridinone series, the effects of various substitutions in ring A depend on the substitution in ring C.[23] On the basis of these results, we propose a molecular model in the naphthyridinone series (Chart 5): the functional groups must be sterically and electrostatically compatible with the environment of the colchicine binding site in tubulin. According to this proposed model, compound **105** (Chart 5) was synthesized and showed potent inhibitory activity against tubulin polymerization with a pIC_{50} value of 6.04[32] (predicted pIC_{50} value of 5.62). Thus, the CoMFA model brings important structural insights to aid the rational design of novel antitubulin agents, and currently, it is being used in the design of new colchicine binding site agents.

Recently, Downing's group determined the structure of the $\alpha\beta$ tubulin heterodimer with Taxol by means of electron crystallography at 3.7 Å resolution.[41] This structure is currently available from the Brookhaven Protein Databank. Unfortunately, much evidence indicates that colchicine and its analogues bind in a different site in the tubulin molecule than Taxol.[29] We plan to use the tubulin structure to predict the putative colchicine-binding site and further employ structure-based approaches to the design of novel tubulin inhibitors. The results of these ongoing studies will be reported in forthcoming publications.

Acknowledgment. This investigation was supported in part by Grant CA 17625 from the National Cancer Institute awarded to K.H.L. A.T. acknowledges a software grant from Tripos Inc. We thank Dr. Susan Morris-Natschke for her critical reading of the manuscript, many valuable suggestions, and assistance.

References

(1) Yang, Z. Y.; Xia, Y.; Brossi, A.; Xia, P.; Lee, K. H. Antitumor agents 198. A concise regiospecific synthesis of 8,8-dimethyl-2H,8H-pyrano[6,5-H]quinolin-2-one and related compounds. *Tetrahedron Lett.* **1999**, *40*, 4505−4506.

(2) Wordenmam, L.; Mitchison, T. J. Dynamics of microtubule assembly in vivo. In *Microtubules*; Hyams, J. S., Lloyd, C. W., Eds.; Wiley-Liss, Inc.: New York, 1994; pp 287−301.

(3) Hamel, E. Antimitotic natural products and their interactions with tubulin. *Med. Res. Rev.* **1996**, *16*, 207−231.

(4) Rowinsky, E. K.; Donehower, R. C. The clinical pharmacology and use of antimicrotubule agents in cancer chemotherapeutics. *Pharmacol. Ther.* **1992**, *52*, 35−84.

(5) Verij, J.; Clavel, M.; Chevalier, B. Palitaxel and docetaxel: not simply two of a kind. *Ann. Oncol.* **1994**, *5*, 495−505.

(6) Hastie, S. B. Interaction of colchicine with tubulin. *Pharmacol. Ther.* **1994**, *51*, 377−401.

(7) Hamel, E.; Ho, H. H.; Kang, G. J.; Lin, C. M. Cornigerine, a potent antimitotic colchicum alkaloid of unusual structure: interactions with tubulin. *Biochem. Pharmacol.* **1988**, *37*, 2445−2449.

(8) Kelly, M.; Hartwell, J. The biological effects and the chemical composition of podophyllin. *J. Natl. Cancer Inst.* **1954**, *14*, 967−1010.

(9) Wang, R. W. J.; Rebhun, L. I.; Kupchan, S. M. Antimitotic and antitubulin activity of the tumor inhibitor steganacin. *Cancer Res.* **1977**, *37*, 3071−3079.

(10) Lin, C. M.; Ho, H. H.; Pettit, G. R.; Hamel, E. Antimitotic natural products combretastatin A-4 and combretastatin A-2: studies on the mechanism of their inhibition of binding of colchicine to tubulin. *Biochemistry* **1989**, *28*, 6984−6991.

(11) Pettit, G. R.; Singh, S. B.; Boyd, M. R.; Hamel, E.; Pettit, R. K.; Schmidt, J. M.; Hogan, F. Antineoplastic agents. 291. Isolation and synthesis of combretastatins A-4, A-5, and A-6 (1a). *J. Med. Chem.* **1995**, *38*, 1666−1672.

(12) Shi, Q.; Chen, K.; Li, L.; Chang, J. J.; Autry, C.; Kozuka, M.; Konoshima, T.; Estes, J. R.; Lin, C. M.; Hamel, E.; McPhail, A. T.; McPhail, D. R.; Lee, K. H. Antitumor agents. 154. Cytotoxic and antimitotic flavonols from *Polanisia dodecandra*. *J. Nat. Prod.* **1995**, *58*, 475−482.

(13) Lin, C. M.; Singh, S. B.; Chu, P. S.; Dempcy, R. O.; Schmidt, J. M.; Pettit, G. R.; Hamel, E. Interaction of tubulin with potent natural and synthetic analogues of the antimitotic agent combretastatin, a structure−activity study. *Mol. Pharmacol.* **1988**, *34*, 200−208.

(14) Hamel, E. Interactions of tubulin with small ligands. In *Microtubule Proteins*; Avila, J., Ed.; CRC Press: Boca Raton, FL, 1990; pp 89−191.

(15) Sun, L.; Hamel, E.; Lin, C. M.; Hastie, S. B.; Pyluck, A.; Lee, K. H. Antitumor agents. 141. Synthesis and biological evaluation of thiocolchicine analogues: N-acyl, N-aroyl, and N-(substituted benzyl)deacetylthiocolchicines as cytotoxic and antimitotic compounds. *J. Med. Chem.* **1993**, *36*, 1474−1479.

(16) Sun, L.; Hamel, E.; Lin, C. M.; Hastie, S. B.; Chang, J. J.; Lee, K. H. Antitumor agents. 139. Synthesis and biological evaluation of thiocolchicine analogues 5,6-dihydro-6(S)-acyloxy- and 5,6-dihydro-6(S)-[(aroyloxy)methyl]-1,2,3-trimethoxy-9-(methylthio)-8H-cyclohepta[a]naphthalen-8-ones as novel cytotoxic and antimitotic agents. *J. Med. Chem.* **1993**, *36*, 544−551.

(17) Shi, Q.; Chen, K.; Verdier-Pinard, P.; Brossi, A.; Hamel, E.; McPhail, A. T.; Lee, K. H. Antitumor agents − Part 184 − Syntheses and antitubulin activity of compounds derived from reaction of thiocolchicone with amines: lactams, alcohols, and ester analogues of allothiocolchicinoids. *Helv. Chim. Acta* **1998**, *81*, 1023−1037.

(18) Shi, Q.; Chen, K.; Chen, X.; Verdier-Pinard, P.; Brossi, A.; Hamel, E.; McPhail, A. T.; Lee, K. H. Antitumor agents. 183. Syntheses, conformational analyses, and antitubulin activity of allothiocolchicinoids. *J. Org. Chem.* **1998**, *63*, 4018−4025.

(19) Shi, Q.; Verdier-Pinard, P.; Brossi, A.; Hamel, E.; Lee, K. H. Antitumor agents − CLXXV. Anti-tubulin action of (+)-thiocolchicine prepared by partial synthesis. *Bioorg. Med. Chem.* **1997**, *5*, 2277−2282.

(20) Shi, Q.; Verdier-Pinard, P.; Brossi, A.; Hamel, E.; McPhail, A. T.; Lee, K. H. Antitumor agents. 172. Synthesis and biological evaluation of novel deacetamidothiocolchicin-7-ols and ester analogues as antitubulin agents. *J. Med. Chem.* **1997**, *40*, 961−966.

(21) Li, L.; Wang, H. K.; Kuo, S. C.; Wu, T. S.; Lednicer, D.; Lin, C. M.; Hamel, E.; Lee, K. H. Antitumor agents. 150. 2′,3′,4′,5′,5,6,7-Substituted 2-phenyl-4-quinolones and related compounds: their synthesis, cytotoxicity, and inhibition of tubulin polymerization. *J. Med. Chem.* **1994**, *37*, 1126−1135.

(22) Li, L.; Wang, H. K.; Kuo, S. C.; Wu, T. S.; Mauger, A.; Lin, C. M.; Hamel, E.; Lee, K. H. Antitumor agents. 155. Synthesis and biological evaluation of 3′,6,7-substituted 2-phenyl-4-quinolones as microtubule agents. *J. Med. Chem.* **1994**, *37*, 3400−3407.

(23) Chen, K.; Kuo, S. C.; Hsieh, M. C.; Mauger, A.; Lin, C. M.; Hamel, E.; Lee, K. H. Antitumor agents. 174. 2′,3′,4′,5,6,7-Substituted 2-phenyl-1,8-naphthyridin-4-ones: their synthesis, cytotoxicity, and inhibition of tubulin polymerization. *J. Med. Chem.* **1997**, *40*, 2266−2275.

(24) Chen, K.; Kuo, S. C.; Hsieh, M. C.; Mauger, A.; Lin, C. M.; Hamel, E.; Lee, K. H. Antitumor agents. 178. Synthesis and biological evaluation of substituted 2-aryl-1,8-naphthyridin-4(1H)-ones as antitumor agents that inhibit tubulin polymerization. *J. Med. Chem.* **1997**, *40*, 3049−3056.

(25) Guan, J.; Zhu, X. K.; Tachibana, Y.; Bastow, K. F.; Verdier-Pinard, P.; Brossi, A.; Hamel, E.; Lee, K. H. Antitumor agents. Part 186. Synthesis and biological evaluation of demethylcolchiceinamide analogues as cytotoxic DNA topoisomerase II inhibitors. *Bioorg. Med. Chem.* **1998**, *6*, 2127−2131.

(26) Guan, J.; Brossi, A.; Zhu, X. K.; Wang, H. K.; Lee, K. H. Oxidation products of phenolic thiocolchicines: ring A quinones and dienones. *Synth. Commun.* **1998**, *28*, 1585−1591.

(27) Guan, J.; Zhu, X. K.; Brossi, A.; Tachibana, Y.; Bastow, K. F.; Verdier-Pinard, P.; Brossi, A.; Hamel, E.; McPhail, A. T.; Lee, K. H. Antitumor agents. 192. Antitubulin effect and cytotoxicity of C(7)-oxygenated allocolchicinoids. *Collect. Czech. Chem. Commun.* **1999**, *64*, 217−228.

(28) Xia, Y.; Yang, Z. Y.; Xia, P.; Bastow, K. F.; Tachibana, Y.; Kuo, S. C.; Hamel, E.; Hackl, T.; Lee, K. H. Antitumor agents 181. Synthesis and biological evalution of 6,7,2′,3′,4′-substituted-1,2,3,4-tetrahydro-2-phenyl-4-quinolones as a new class of antimitotic antitumor agents. *J. Med. Chem.* **1998**, *41*, 1155−1162.

(29) Shi, Q.; Chen, K.; Morris-Natschke, S.; Lee, K. H. Recent progress in the development of tubulin inhibitors as antimitotic antitumor agents. *Curr. Pharm. Des.* **1998**, *4*, 219−248.

(30) ter Haar, E.; Rosenkranz, H. S.; Hamel, E.; Day, B. W. Computational and molecular modeling evaluation of the structural basis for tubulin polymerization inhibition by colchicine site agents. *Bioorg. Med. Chem.* **1996**, *4*, 1659−1671.

(31) Cho, S. J.; Tropsha, A. Cross-validated R^2-guided region selection for comparative molecular-field analysis: a simple method to achieve consistent results. *J. Med. Chem.* **1995**, *38*, 1060−1066.

(32) Zhang, S. X.; Bastow, K. F.; Tachibana, Y.; Kuo, S. C.; Hamel, E.; Mauger, A.; Narayanan, V. L.; Lee, K. H. Antitumor agents. 196. Substituted 2-thienyl-1,8-naphthyridin-4-ones: their synthesis, cytotoxicity, and inhibition of tubulin polymerization. *J. Med. Chem.* **1999**, *42*, 4081−4087.

(33) Gaillard, P.; Carrupt, P. A.; Testa, B.; Schambel, P. Binding of arylpiperazines, (aryloxy)propanolamines, and tetrahydropyridylinldoles to the 5-HT1A receptor: contribution of the molecular lipophilicity potential to three-dimensional quantitative structure-affinity relationship models. *J. Med. Chem.* **1996**, *39*, 126−134.

(34) *Sybyl User's Manual Version* 6.5; Tripos, Inc.: St. Louis, MO, 1998.

(35) Cho, S. J.; Tropsha, A., Suffness, M.; Cheng, Y. C.; Lee, K. H., Antitumor agents. 163. Three-dimensional quantitative structure−activity relationship study of 4′-*O*-demethylepipodophyllotoxin analogues using the modified CoMFA/q(2)-GRS approach. *J. Med. Chem.* **1996**, *39*, 1383−1395.

(36) Brossi, A.; Boye, O.; Muzaffar, A.; Yeh, H. J. C.; Toome, V.; Wegrzynski, B.; George, C. *aS*,7*S*-Absolute configuration of natural (−)-colchicine and allocongeners. *FEBS Lett.* **1990**, *262*, 5−7.

(37) Brossi, A.; Yeh, H. J.; Chrzanowska, M.; Wolff, J.; Hamel, E.; Lin, C. M.; Quinn, F.; Suffness, M.; Silverton, J. Colchicine and its analogues: recent findings. *Med. Res. Rev.* **1988**, *8*, 77−94.
(38) Yeh, H. J.; Chrzanowska, M.; Brossi, A. The importance of the phenyl-tropolone *aS* configuration in colchicine's binding to tubulin. *FEBS Lett.* **1988**, *229*, 82−86.
(39) Berg, U.; Bladh, H. The absolute configuration of colchicine by correct application of the *CIP* rules. *Helv. Chim. Acta* **1999**, *82*, 323−325.
(40) Brossi, A.; Lee, K. H.; Yeh, H. J. C. Axial configuration of optically active colchicinoids and allocolchicinoids: A correction. *Helv. Chim. Acta* **1999**, *82*, 1223−1224.
(41) Nogales, E.; Wolf, S. G.; Downing, K. H. Structure of the alpha beta tubulin dimer by electron crystallography. *Nature* **1998**, *391*, 199−203.

JM990333A